Korean J. Chem. Eng., **29**(9), 1203-1210 (2012)
DOI: 10.1007/s11814-012-0011-6

Electro-Fenton treatment of synthetic organic dyes: Influence of operational parameters and kinetic study

Prabir Ghosh†, Lalit Kumar Thakur, Amar Nath Samanta, and Subhabrata Ray

Department of Chemical Engineering, IIT Kharagpur, Kharagpur 721302, India
(*Received 11 November 2011 • accepted 6 February 2012*)

Abstract–This work investigates oxidative decolorization of two different dyes, Methylene blue and Titan yellow in aqueous solution using an environmentally friendly advanced electro-chemical oxidation (electro-Fenton) process. The effect of operating conditions like H_2O_2 concentration, current density, initial dye concentration was studied in a batch stirred cell. Individual decolorization decay kinetics for both dyes was investigated. The second-order absolute rate constants (L mol^{-1} s^{-1}) between hydroxyl radical and dye have been calculated from experimental data by fitting it to the decolorization model. The apparent kinetic constants, k_{app} (s^{-1}) for Methylene blue and Titan yellow dye decolorization were also determined. The experimental data showed a good fit to the theoretical model, which can predict data in a wide range of % dye decolorization. This process also reduces COD of the dye solution, and the unit energy demand (UED) in kWh/kg COD removed for different electrical current has been reported.

Key words: Electro-Fenton Process, Hydroxyl Radicals, Environmental Pollution, Modeling, Kinetics, Rate Constants

INTRODUCTION

Synthetic dyes discharged from different industries such as textile, paper and cosmetics are characterized by intense color and high organic concentration. The discharge of dye effluents at high concentration presents a serious environmental pollution problem because many dyes are toxic and recalcitrant to biodegradation [1,2]. The highest rate of toxicity was found amongst basic and diazo direct dyes [3,4]. Dye contamination in wastewater causes problems in several ways: color interferes with penetration of sunlight into waters, retards photosynthesis and inhibits the growth of aquatic biota [5-8]. Some of the dyes are characterized by the presence of azo groups (-N=N-) in combination with aromatic systems. Because of the chemical and light stable characteristics of the azo group, conventional wastewater treatment methods, coagulation, adsorption and flocculation, have been proved to be non-destructive or ineffective for the efficient degradation of several such dye compounds [9,10]. Although Methylene blue is not strongly hazardous, but it can cause several harmful effects such as nausea, vomiting, shock, cyanosis, jaundice, and quadriplegia and tissue necrosis in humans [11,12]. It is necessary to treat dye effluents prior to their discharge into the receiving water stream to meet the environmental regulations.

Fenton and the electro-Fenton processes can be represented as $M^{n+}+H_2O_2 \rightarrow M^{(n+1)+}+HO^-+HO^\bullet$ or $M^{(n+1)+}+H_2O_2 \rightarrow M^{n+}+HO_2^\bullet+H^+$ where M is a transition metal, e.g., Fe, Cu, etc. The reaction clearly states that the transition metal is being oxidized by hydrogen peroxide, resulting in formation of highly reactive species hydroxyl radical with oxidation potential of 2.8 V, which can effectively oxidize the organic molecules with the rate constants usually in the order of 10^7-10^{10} L mol^{-1} s^{-1} [13]. Dye oxidation in a simplified form, can be represented by - $HO^\bullet$+dye→intermediates→harmless species (CO_2, H_2O etc).

However, formation of metal hydroxide sludge is a major disadvantage in the conventional Fenton process that involves continuous addition of metal salt.

In this work, two synthetic dyes, methylene blue (MB) basic dye and Titan yellow (TY) azo-dye were chosen as representative model pollutants due to their common use. Table 1 shows some characteristics of MB and TY.

Table 1. Characteristics of MB and TY

Parameter	Methylene blue (MB)	Titan yellow (TY)
MW (g/mol)	355.89	695.73
Formula	$C_{16}H_{18}N_3SCl \cdot 2H_2O$	$C_{28}H_{19}N_5Na_2O_6S_4$
Wavelength for max. adsorptivity	664 nm	402 nm
Color index (C.I)	52015	19540

A modification of the classical Fenton process by electrochemical dissolution of Fe, supplying the Fe^{2+} ion to the reactions, is called electro-Fenton method. This process has the advantage of in situ generation of Fe^{2+} by passing of direct current between suitable electrodes, thus avoiding the need for addition of iron salt [14]. Controlling the cell current it regulates the addition rate of Fe^{2+}. Work has also been reported on electro-generation of Fe^{2+} or H_2O_2 to treat synthetic or industrial wastewater [15-17]. This new hybrid technology employing electricity as clean energy source does not produce secondary pollutants and is compatible with the environment [18]. In recent years, electrochemical methods have been effectively studied for destruction of various dyes [19-21].

As Fe^{2+} is obtained from the anode, by electrochemical dissolution, the sacrificial anode needs to be replaced from time to time, and this is a limitation. In addition, Fe^{2+} also gets into the solution by chemical dissolution, as the reaction takes place in acidic pH,

†To whom correspondence should be addressed.
E-mail: prabirghosh2007@yahoo.co.in

typically around 3. A graphite cathode has been used in this work. It may be pointed out that during the electro-Fenton treatment of dyes, a certain amount of iron was continuously dissolved into the wastewater from the cast iron anodes, according to Faraday's law [22]. The dissolved fraction of iron along with the externally added H_2O_2 functions much like Fenton's reagent [23,24].

The generation of Fe^{2+} ion in the solution by different processes is explained below-

Electrochemical Dissolution: When current passes, the iron anode oxidizes to ferrous iron as follows:

$$Fe \rightarrow Fe^{2+} + 2e^-$$

Faraday's law gives the rate at which electrode is being corroded or the rate at which Fe^{2+} is generated in the solution. This rate is given by the expression

$$\frac{dC_{Fe^{2+}}}{dt} = \frac{Ai}{n_e F V} \quad (1)$$

where, A is electrochemical surface area, i is the current density, V is the volume of the reactor, is the number of electrons transferred, F is the Faraday constant

Chemical Dissolution: Iron electrodes are prone to chemical dissolution by H^+ attack. Current efficiency studies do support this.

$$Fe + 2H^+ \rightarrow Fe^{2+} + H_2$$

The kinetics of this reaction is expressed as corrosion current, $I_{corr} = j_0 A_i \exp(fE/4)$ and the iron dissolution rate by H^+ attack is given by

$$\frac{dC_{Fe^{2+}}}{dt} = \frac{j_0 A_i e^{\left(\frac{fE}{4}\right)}}{n_e F V} \quad (2)$$

where, j_0 is the exchange current density of H^+ attack on iron ($j_0 = 1\times10^{-6}$ A cm^{-2}), A_i is the area of iron surface, E is the cell potential of the corrosion couple (Fe/Fe^{2+}), given by:

$$E\ (\text{Volts}) = 0.44 - 0.059 \times \text{pH}, \text{ is a constant given by, } f = \frac{F}{RT} = \frac{1}{25.6\ \text{mV}}$$

Although there are some reports on application of similar process for degradation of organic pollutants such as benzene ring compounds [25-27], studies on degradation kinetics of dyes are limited [28-32]. The aim of the present work is to find second-order absolute rate constants (L mol^{-1} s^{-1}) between hydroxyl radical ($^{\bullet}OH$) and dyes in a stirred batch cell by electro-Fenton process. Also, the apparent rate constants (s^{-1}) for both the dyes were determined. This information may be used for modeling, design and optimization of chemical reactors used for the degradation of these dyes. Effect of variation of operational parameters such as H_2O_2 concentration, current density and initial dye concentration on decolorization efficiency have been investigated.

MATERIALS AND METHODS

1. Reagents

Methylene blue and Titan yellow dyes were procured from M/s Loba Chemie Pvt. Ltd., Mumbai, India. Dye solutions of required concentration (mg L^{-1}) were prepared with distilled water. H_2O_2 (50% v/v) was supplied by M/s Merck Ltd, Mumbai, India. NaCl used for improving conductivity of solution was of Guaranteed Reagent (GR) grade and was obtained from M/s Merck Ltd., Mumbai, India.

2. Analytical Methods

During experiments, the pH was determined by a digital pH meter model CL 46$^+$ from M/s Toshcon Industries Pvt. Ltd., Hardwar, India. Conductivity of the solution was measured by a digital conductivity meter model No 611E from M/s El Products, Parwanoo, India. Power supplied to the electrochemical cell was from a DC regulated power source, Model 93C, M/s Testronix (India). The power source was set at constant current mode. Chemical oxygen demand (COD) of the initial dye solution and treated dye solution were measured by "open reflux method" according to the standard methods for the examination of water and wastewater [33]. Sample containing H_2O_2 may interfere with the COD test since the dichromate ions can react with H_2O_2 in an acidified solution [34]. To remove residual H_2O_2 in the samples, the samples were pretreated with NaOH to raise the pH above 7 before COD measurement. At this stage H_2O_2 decomposes to oxygen and water and loses its oxidation capability [35,36], thus preventing the interference in the reaction. At higher pH, Fe^{2+} gets precipitated as $Fe(OH)_3$. For this reason, COD measurements were performed only after the coagulation stage.

Copncentration of dyes in solution at different time interval was obtained by measuring absorbance at maximum absorption wavelength (664 nm for MB and 402 nm for TY), and decolorization decay was computed from calibration curve prepared earlier. A Chemito (India) UV-VIS Spectrophotometer (model - VS-2100) was employed for absorbance measurements using quartz cell of path length 1 cm.

The equation for the calibration curve of Methylene blue dye was found to be $Y_{MB} = 0.17252\ X_{MB}$; $R^2 = 0.9985$; where Y_{MB} is the solution absorbance at 664 nm and X_{MB} is the concentration of MB in mg L^{-1}. Calibration was done in the range of concentration 0 to 10 mg L^{-1} for MB dye and 0 to 25 mg L^{-1} for TY dye. The equation for calibration curve of TY dye is found to be: $Y_{TY} = 0.01995\ X_{TY}$; $R^2 = 0.9988$; where Y_{TY} is the solution absorbance at 402 nm and X_{TY} is the concentration of TY in mg L^{-1}. The normalized decolorization decay, expressed in terms of (A/A_0), was calculated, where A is the absorbance determined at the maximum wavelength of the dye and A_0 is the initial absorbance of dye solution at this wavelength.

EXPERIMENTAL

Batch experiments were performed in a cylindrical electrolytic cell (Borosil glass) of 1 lit containing 0.8 lit of dye solution equipped with a graphite cathode (75 mm×30 mm×6 mm) and iron anode (128 mm×57 mm×0.5 mm). The effective anode area was 23.22 cm^2. The parallel electrode pair was arranged vertically with 23 mm spacing and held from the top with clamps. Electrodes were cleaned with emery paper (No. P320) between the successive runs and then washed with H_2SO_4 solution (5% v/v) to reduce the effects of proceeding experiments. The porous graphite cathode was also kept dipped in the dye solution for minimum 12 hrs to saturate it with dye, so that the effect of dye absorption due to porosity could be minimized. Conductivity of the solution was improved above 1 mS cm^{-1} by adding 1,000 mg L^{-1} NaCl. This concentration of salt is quite common in the textile industry for fixing the color. Initial pH

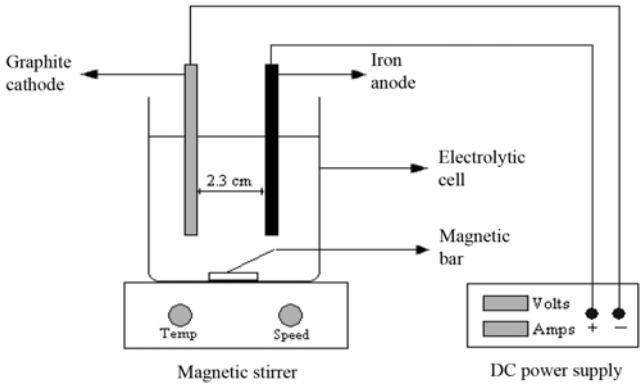

Fig. 1. Schematic diagram of experimental set-up.

of the solution was adjusted to pH 3 using 2 N H_2SO_4. Required amount of H_2O_2 was added to the electrolytic cell, and then the DC power source was switched on in constant current mode. Cell current density was varied by changing the cell voltage. The solution was agitated with a magnetic stirrer plate (Model-MC02, Tarsons India Ltd.) during electro-Fenton process at a specific speed (250 RPM) all the time. All experiments were carried out at ambient temperature, around 28 to 30 °C. Small amount of sample liquid was drawn as necessary, and the oxidation reaction was stopped by adding NaOH to the sample. The samples were then filtered through filter paper (Whatman No. 42) to remove any precipitate before analysis. Each experiment was repeated minimum twice. A schematic diagram of the cell along with other arrangements is shown in Fig. 1.

Considering the selection of process parameters, it is expected that dye should degrade in around 60 min. In few cases, when it was not degrading within this time, the process parameter set was changed so as to degrade around 60 min.

RESULTS AND DISCUSSION

1. Effect of Experimental Parameters on the Dye Degradation

To study the effect of process parameters on the performance of the electro-Fenton process, several sets of experiments were performed covering the following: (i) effect of initial dye concentration, (ii) effect of H_2O_2 concentration for both dyes, and (iii) effect of current density for both the dyes.

1-1. Effect of Initial Concentration of Dye

The effect of initial concentration of dye (MB) on decolorization decay was investigated and the results are in Fig. 2. During the experiment, the proportion of H_2O_2 to MB was kept same. At higher initial MB concentration, the decolorization decay rate was lower. More than 98% decolorization was achieved with 100 mg L^{-1} MB initial dye concentration after 60 min of treatment time, whereas for initial MB concentration of 300 mg L^{-1}, less than 90% decolorization was observed for the same time duration. These experiments were conducted at initial pH 3 as the electro-Fenton activity is highest at this pH according to the literature [37,38] for degradation of organic pollutants by Fenton-related method. At pH above 3, the decolorization degree decreases significantly mainly because the dissolved fraction of iron species diminishes with increasing pH [39]. At pH below 3, hydrogen peroxide forms oxonium ion

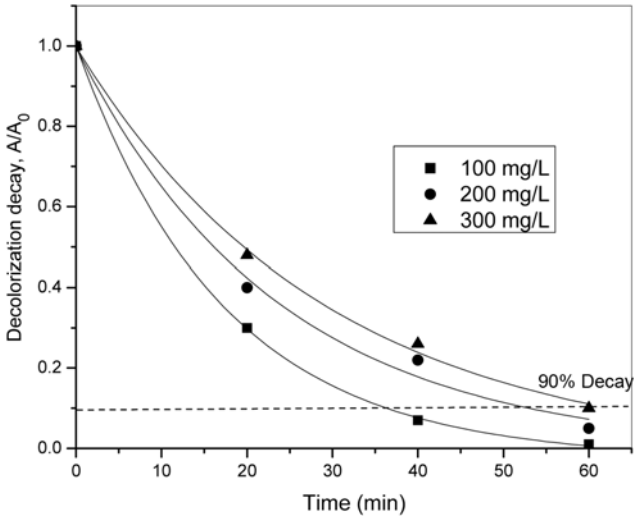

Fig. 2. Normalized decolorization of Methylene blue dye at different initial concentration with same pH and current density values (Current density: 4.31 mA cm^{-2}, pH: 3.00, H_2O_2 concentration for 100, 200 and 300 mg L^{-1} dye: 1 mM, 2 mM and 3 mM.

($H_3O_2^+$) by solvating a proton that reduces the reactivity of H_2O_2 towards electro-generated ferrous ions and effectively fewer hydroxyl radicals are produced at lower pH [40]. The hydroxyl radicals generated are the main species responsible for decolorization of dye. As the proportion of the hydroxyl radical to the dye to be decolorized falls with increasing concentration of dye, effectively a lower fraction of dye gets decolorized. These experiments were not repeated with Titan Yellow as the outcome expected is similar.

1-2. Effect of Initial Concentration of H_2O_2

Fig. 3 & 4 show the effect of initial H_2O_2 concentration on MB and TY dye decolorization decay. The extent of both MB and TY

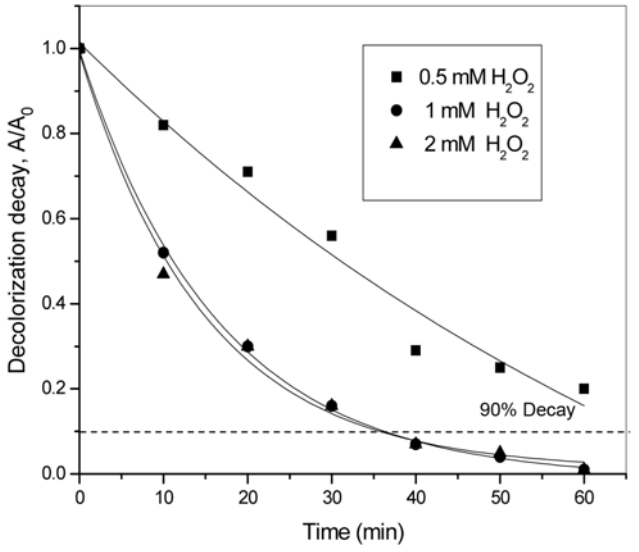

Fig. 3. Normalized decolorization of Methylene blue dye at different initial H_2O_2 concentration with same pH and current density values (Dye concentration: 100 mg L^{-1}, Current density: 4.31 mA cm^{-2}, pH: 3).

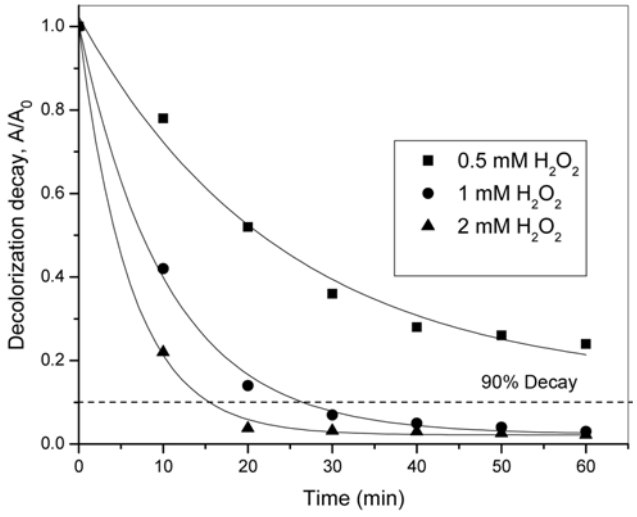

Fig. 4. Normalized decolorization of Titan yellow dye at different initial H_2O_2 concentration with same pH and current density values (Dye concentration: 100 mg L^{-1}, Current density: 4.31 mA cm^{-2}, pH: 3).

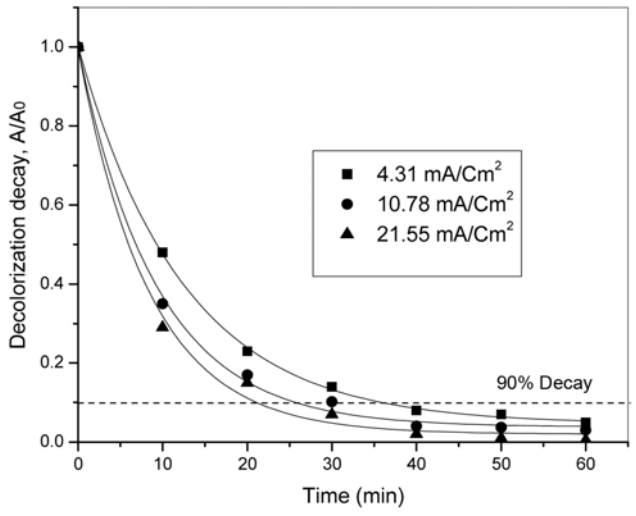

Fig. 5. Normalized decolorization of Methylene blue dye at different initial current density (Dye concentration: 500 mg L^{-1}, pH: 3, Initial H_2O_2: 5 mM).

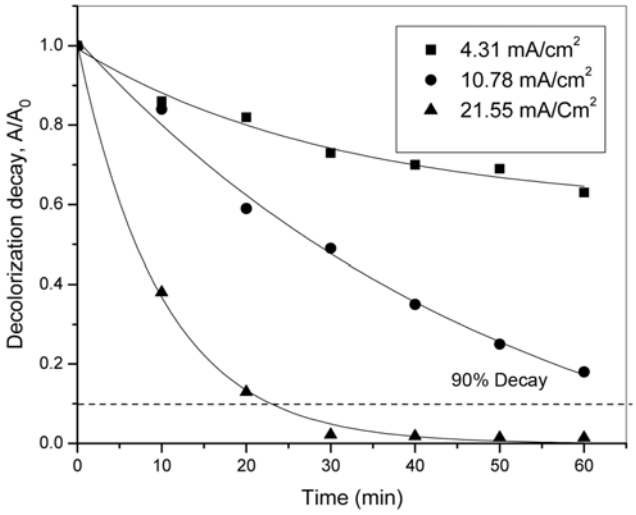

Fig. 6. Normalized decolorization of Titan yellow dye at different initial current density (Dye concentration: 500 mg L^{-1}, pH: 3, Initial H_2O_2: 5 mM).

decolorization increased (79.73% to 98% for MB and 75.8% to 96% for TY) as the H_2O_2 concentration increases from 0.5 mM to 1 mM. Enhanced decolorization of dyes was due to the increased availability of $^{\bullet}OH$ radicals generated from higher amount of hydrogen peroxide [41]. Further increase in H_2O_2 concentration from 1 mM to 2 mM causes no significant change in decolorization decay. This is possibly because at higher H_2O_2 concentration scavenging of $^{\bullet}OH$ radicals occurs according to the following reactions: $H_2O_2+{}^{\bullet}OH \rightarrow H_2O+HO_2^{\bullet}$ and $HO_2^{\bullet}+{}^{\bullet}OH \rightarrow H_2O+O_2$ [42,43]. The results indicate that when the H_2O_2 concentration is 1 mM, MB and TY decolorization was 98% and 96% for treatment time of 60 minutes. Comparison of decolorization decay at higher concentrations of H_2O_2 shows that decolorization of MB is slightly higher than that of TY, when the initial mass concentrations are same.

1-3. Effect of Current Density

The efficiency of the process depends on electric current since it is an important operating parameter in the electro-Fenton process. The dissolution rate of Fe^{2+} from anode is mainly dependent on current, which is responsible for decolorization of dyes. Therefore, the effect of current on decolorization decay is investigated in this study [44]. Fig. 5 & Fig. 6 show the effect of current density on MB and TY dye decolorization. Higher decolorization efficiency corresponding to higher current density depicted in figures is due to higher electrogeneration/availability of Fe^{2+} from the iron anode. While a DC current is applied to the electrochemical reactor, the amount of Fe^{2+} ions dissolved from the sacrificial iron anode increases through this reaction ($Fe \rightarrow Fe^{2+}+2e^-$). This phenomenon is very crucial to enhance the decolorization decay, as it helps propagate the basic Fenton reaction [45]. Decolorization was poor initially because of unavailability of sufficient amount of Fe^{2+} ion in solution, as expected because the oxidizing power of hydrogen peroxide is not enough to destroy the dye molecules [46]. The decolorization in 60 min time was 94.26%, 96.92% and 99.5% for current density of 4.31, 10.78 and 21.55 mA cm^{-2}, respectively, for MB dye. For TY dye, decolorization obtained was 36.84%, 81.62% & 98.58% for current density of 4.31, 10.78 and 21.55 mA cm^{-2}, respectively. In the case of TY, the reduction in concentration over the same time duration is less with the same set of operating conditions pointing at lower extent of decolorization of TY compared to MB dye, for same initial mass concentration. The dyes considered here are large and complex molecules and possibly lead to intermediates in the first step of degradation. These intermediates undergo degradation simultaneously with the dye molecules, competing for the oxidizing radicals/oxidizing agents. TY molecules being larger and more complex than MB possibly leads to more intermediates competing for the available oxidants, and this makes degradation of TY slower compared to MB.

2. Simultaneous Degradation of Dyes in Mixture

Fig. 7 shows the progress of degradation for dye mixture consisting of TY and MB in same mass concentrations. In case of individual/pure dye degradation with 500 mg L^{-1} initial concentra-

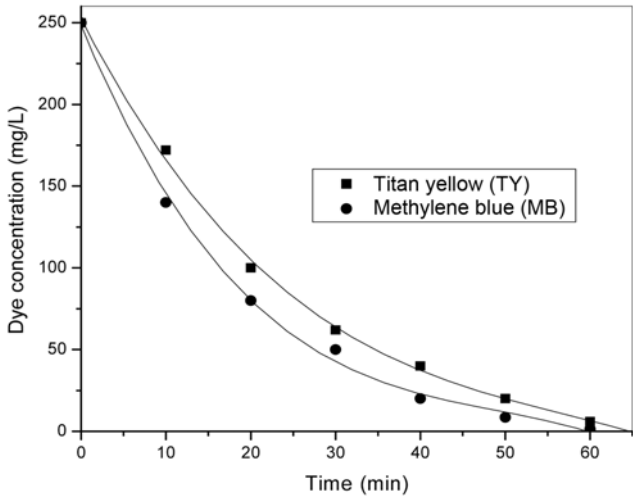

Fig. 7. Effect of presence of another dye (Dye conc: 250 mg L^{-1} TY & 250 mg L^{-1} MB, Initial pH: 3, Initial H_2O_2: 5 mM, Current density: 10.78 mA cm^{-2}).

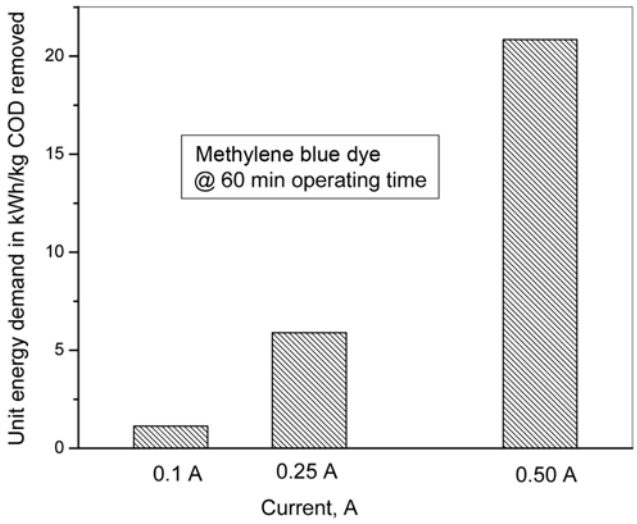

Fig. 8. Energy consumption based on electric current during electro-Fenton treatment, 500 mg L^{-1} dye concentration.

tion and rest of the parameters kept same (Initial pH: 3, Initial H_2O_2: 5 mM, Current density: 10.78 mA cm^{-2}), MB and TY degradation in 60 min was 96.92% and 81.62%, respectively. Degradation over a period of 60 min in a mixture (initial concentration 250 mg L^{-1} for each dye) with same process parameters led to 99.4% and 97.4% degradation for MB and TY, respectively. For the same concentration of two dyes in mixture, MB experienced higher degradation compared to TY due to reasons already explained.

3. Unit Energy Demand (UED) of the Electro-Fenton Process

Energy consumption is electrical energy spent to reduce unit amount of COD, expressed in kWh/kg COD removed in time t hr. The efficiency of the energy can be explained as consumed energy per unit contaminant reduced. Unit energy demand for each m^3 of wastewater of the electro-Fenton process was calculated by the following formula: UED=$(SEC_{(t)}/(C_i \times \eta_{(t)}))\times 100$ where C_i is the initial concentration of COD in kg/m^3, η is the COD reduction percentage, SEC is the specific energy consumption in kWh/m^3, SEC=$(V\times I\times t)/(10^3\times v)$ where V is the average cell voltage in volt, was taken for calculating specific energy consumption during electrolysis, I is the cell current, A; and v is the volume of solution (0.8 L).

COD reduction for MB dye has been considered in this study. Electro-Fenton process employed greatly enhanced COD removal. Fig. 8 shows data generated at different current density values, 4.31 mA cm^{-2} (0.1 A), 10.78 mA cm^{-2} (0.25 A) and 21.55 mA cm^{-2} (0.50 A). The initial COD was 670 mg L^{-1} for 500 mg L^{-1} of MB. It can be seen that with increase of cell current, UED also increases. At 4.31 mA cm^{-2}, 10.78 and 21.55 mA cm^{-2}, in 60 min, the corresponding COD reductions are 68, 75 and 80%. These correspond to UED of 1.14, 5.89 and 20.85 kWh/kg COD removed. Although at a minimum current of 0.1 A, the energy requirement was lower, i.e., 1.14 kWh/kg COD removed, but the COD reduction was relatively low (68%) compared to 80% at 0.5 A. This study also proved that at higher current mineralization efficiency was higher.

4. Kinetic Modeling of the Process

4-1. Determination of Absolute Rate Constants and Apparent Rate Constants

The Electro-Fenton process is efficient for decolorizing dyes in aqueous solution. In all cases, dye concentrations decrease practically exponentially. The decolorization pattern follows a pseudo-first order reaction kinetics between dye molecules (MB & TY) with hydroxyl radicals. As hydroxyl radicals are of very short life time species, the concentration of hydroxyl radicals can be assumed as steady state value.

$$-d[dye]/dt=k_{dye}[dye][^{\bullet}OH]=k_{app}[dye]$$

Table 2. Second-order absolute rate constants (k_2, k_3) and k_{app} for Methylene blue

Exp. no.	Dye conc., mg L^{-1}	pH	H_2O_2, mM	Current density, mA cm^{-2}	k_2 (L mol^{-1} s^{-1})	k_3 (L mol^{-1} s^{-1})	k_{app} (s^{-1}) ($\times 10^3$)	R^2 for k_{app}
MB-1	100	3.0	1.0	4.31	66.70	7.9048×10^8	1.05	0.9927
MB-2	100	3.0	0.5	4.31	16.704	5.9107×10^8	0.51	0.9516
MB-3	100	3.0	2.0	4.31	21.305	2.3451×10^8	0.89	0.9859
MB-4	500	3.0	5.0	4.31	7.3235	2.0673×10^8	0.70	0.9371
MB-5	500	3.0	5.0	10.78	10.933	2.5579×10^8	0.85	0.9385
MB-6	500	3.0	5.0	21.55	6.2405	4.3571×10^8	1.46	0.9939
MB-7	200	3.0	2.0	4.31	16.276	2.1907×10^8	0.74	0.9564
MB-8	300	3.0	3.0	4.31	16.093	2.3702×10^8	0.55	0.9579

Table 3. Second-order absolute rate constants (k_2, k_3) and k_{app} for titan yellow

Exp. no.	Conc., mg L^{-1}	pH	H_2O_2, mM	Current density, mA/cm^2	k_2	k_3	k_{app} (s^{-1}) ($\times 10^3$)	R^2 for k_{app}
TY-1	100	3.0	0.5	4.31	3.7132	1.683×10^8	0.54	0.9816
TY-2	100	3.0	1.0	4.31	7.9723	2.997×10^8	1.04	0.9511
TY-3	100	3.0	2.0	4.31	3.3768	7.920×10^8	0.80	0.7652
TY-4	500	3.0	5.0	4.31	0.0009	1.056×10^8	0.10	0.9595
TY-5	500	3.0	5.0	10.78	0.0007	3.629×10^8	0.5	0.9953
TY-6	500	3.0	5.0	21.55	7.9809	6.6533×0^8	1.11	0.8093

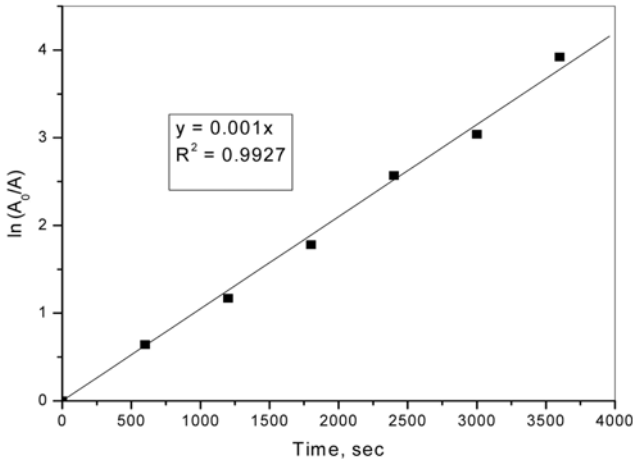

Fig. 9. Determination of apparent rate constant for MB-1.

Where $k_{app}=k_{dye}$ [•OH] is the apparent rate constant (s^{-1}) and k_{dye} is the second-order absolute rate constant (L mol^{-1} s^{-1}). The value of k_{app} depends on the initial operating conditions, and the dependence of k_{app} on the operating conditions can be found by performing independent experiments, changing each parameter at a time, after appropriate linearization of the data. Assuming a first-order kinetic for the decolorization of dyes, the apparent rate constants were determined from the slope of concentration versus time plot in accordance with the equation $\ln([dye]_0/[dye]_t)=k_{app}$ t. These rate constants for Methylene blue and Titan yellow decolorization for different reactions are shown in Table 2 and Table 3, respectively. One sample plot for determining apparent rate constants is given below in Fig. 9.

2. Absolute Rate Constants are Estimated by the Following Model

The electro-Fenton decolorization process involves a number of intermediate reactions. Oxidation of the MB dye by electro-Fenton's reagent, if assumed to be a single step mineralization, then the reaction set for the system is:

$$H_2O_2 + Fe^{2+} \xrightarrow{k_1} Fe^{3+} + OH^- + OH^\bullet \quad (3)$$

$$MB + H_2O_2 \xrightarrow{k_2} MB_{OX} \quad (4)$$

$$MB + OH^\bullet \xrightarrow{k_3} MB_{OX} \quad (5)$$

$$H_2O_2 + OH^\bullet \xrightarrow{k_4} HO_2^\bullet + H_2O \quad (6)$$

$$OH^\bullet + Fe^{2+} \xrightarrow{k_5} Fe^{3+} + OH^- \quad (7)$$

$$Fe^{3+} + H_2O_2 \xrightarrow{k_6} H_2O_2 + H^+ + HO_2^\bullet \quad (8)$$

$$Fe^{3+} + HO_2^\bullet \xrightarrow{k_7} O_2 + Fe^{2+} + H^+ \quad (9)$$

The steady state balances for the different species, from the above reactions are given by

$$\frac{d[HO_2^\bullet]}{dt} = k_4[H_2O_2][OH^\bullet] + k_6[Fe^{3+}][H_2O_2] - k_7[Fe^{3+}][HO_2^\bullet]$$

$$\frac{d[Fe^{2+}]}{dt} = -k_1[H_2O_2][Fe^{2+}] - k_5[OH^\bullet][Fe^+] + k_6[Fe^{3+}][H_2O_2] + k_7[Fe^{3+}][HO_2] + j\times3.0056\times10^{-4} \times\exp^{(4.28182-0.5742\times pH)} + i\times6.48\times10^{-6}$$

$$\frac{d[H_2O_2]}{dt} = -k_1[H_2O_2][Fe^{2+}] - k_2[MB][H_2O_2] - k_4[H_2O_2][OH^\bullet] - k_6[Fe^{3+}][H_2O_2]$$

$$\frac{d[MB]}{dt} = -k_2[MB][H_2O_2] - k_3[MB][OH^\bullet]$$

$$\frac{d[Fe^{3+}]}{dt} = k_1[H_2O_2][Fe^{2+}] + k_5[OH^\bullet][Fe^{2+}] - k_6[Fe^{3+}][H_2O_2] - k_7[Fe^{3+}][HO_2^\bullet]$$

$$\frac{d[HO_2^\bullet]}{dt} = k_4[H_2O_2][OH^\bullet] + k_6[Fe^{3+}][H_2O_2] - k_7[Fe^{3+}][HO_2^\bullet]$$

Solution of this set of ODEs provides the concentration of the different species with time.

This ODE set is solved simultaneously in MATLAB with appropriate set of initial conditions, concentration of different species. Literature [47] reports the following values of rate constants of the reactions involved in the process:

$k_1=63.0$ L mol^{-1} s^{-1} $\quad k_2<10^2$ L mol^{-1} s^{-1}
$k_3=10^7$-10^{10} L mol^{-1} s^{-1} $\quad k_4=3.3\times10^7$ L mol^{-1} s^{-1}
$k_5=3.2\times10^8$ L mol^{-1} s^{-1} $\quad k_6=3\times10^{-3}$ L mol^{-1} s^{-1}
$k_7=2.0\times10^3$ L mol^{-1} s^{-1}

MATLAB function 'ODE15S' based on gear's method is used to solve the above set of differential equations when all k values and the initial conditions of the experiment are known. 'LSQNONLIN' function with 'modified Marquardt-Levenberg method' option is used to minimize the sum of the square of the percentage deviation values between the experimental concentrations of dye and the model predicted values and determine the values of k_2 and k_3.

Initial conditions of one of the experiments, MB-1, are shown below as a typical example.

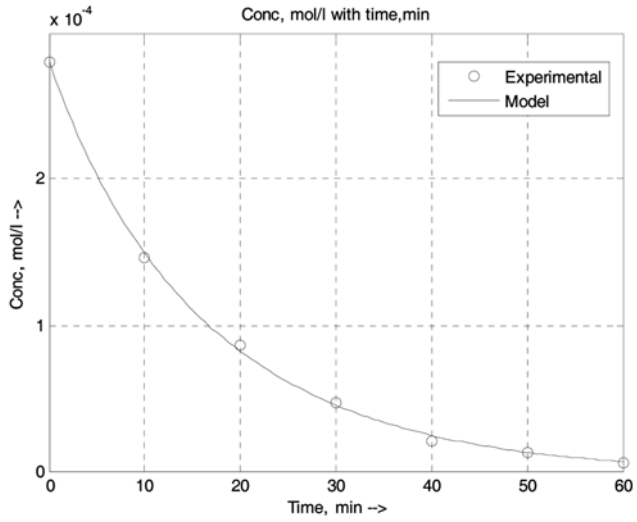

Fig. 10. Experimental and model predicted concentration for expt. MB-1.

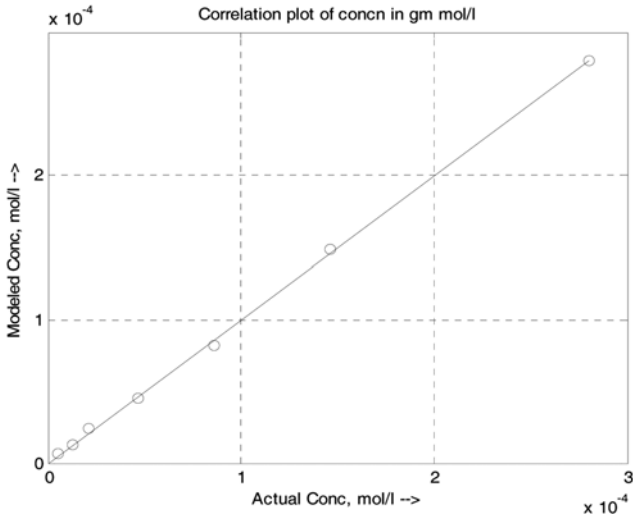

Fig. 11. Concentration correlation plot for expt. MB-1.

$[MB]_0$: 100 mg L^{-1} [2.80×10^{-4} gmol L^{-1}]		$[H_2O_2]_0$: 1 mM [1×10^{-3} gmol L^{-1}]	
$[Fe^{2+}]_0$	: 0	$[Fe^{3+}]_0$	: 0
$[^{\bullet}OH]_0$	: 0	$[HO_2^{\bullet}]_0$	: 0

The experimental results and the model predicted values of Methylene blue concentration for MB-1 are shown in Fig. 10 & 11. Model predicted concentration of $^{\bullet}OH$ radical, Fe^{2+} is shown in Fig. 12 & Fig. 13.

The best-fit second order rate constants (L mol^{-1} s^{-1}) for the experiment MB-1 are

k_2=66.7 and k_3: 7.91×10^8

The rate constants were also calculated from the data of other experiments with MB and also for TY. Since the corresponding plots have similar nature, those are not presented here.

The 2nd order reaction rate constants (k_2 and k_3) as well as the apparent rate constant (k_{app}) obtained from different experiments with MB along with other experimental conditions are presented in Table 2. Table 3 shows the reaction rate constants for TY. It is also seen in Table 2 and Table 3 that at constant pH and current density there is an increasing trend in "k" values (from 5.9107×10^8 to 7.9048×10^8 for MB and 1.683×10^8 to 2.997×10^8 for TY) with increase in H_2O_2 concentration from 0.5 mM to 1 mM. It is also evident that with increase in current density, reaction rate constant (k_3) value increased significantly at constant pH and H_2O_2.

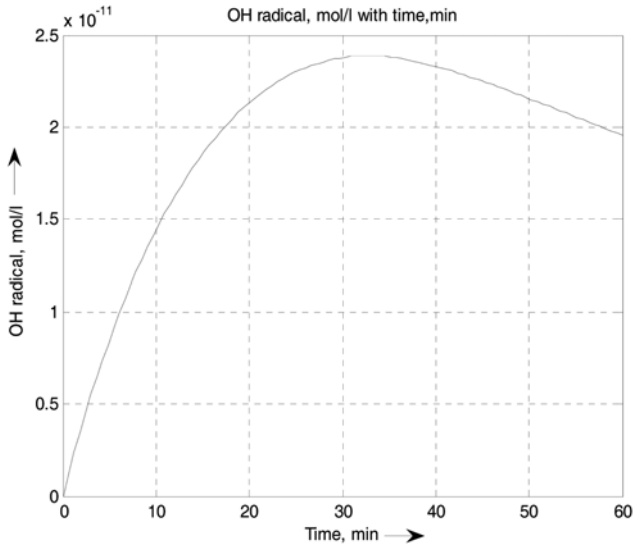

Fig. 12. Model predicted $^{\bullet}OH$ radical concentration for expt. MB-1.

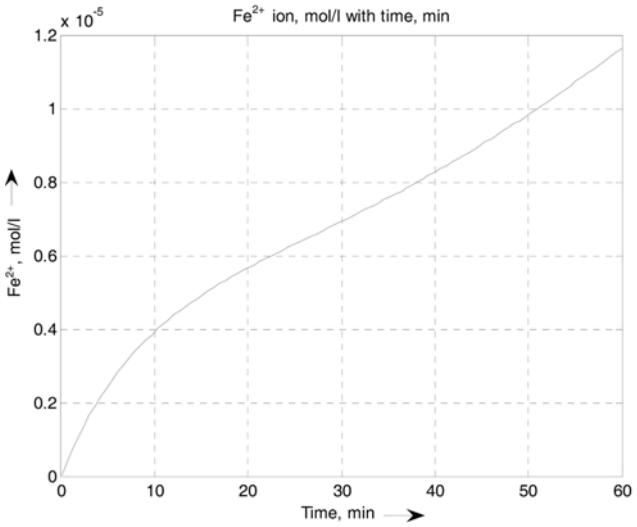

Fig. 13. Model predicted Fe^{2+} concentration for expt MB-1.

CONCLUSIONS

The present study demonstrated that commercial synthetic dyes, Methylene blue and Titan yellow, could be degraded effectively by electro-Fenton process. The experimental results under different operating conditions showed that the % degradation was influenced by H_2O_2 concentration, current density and initial dye concentration. It was found that degradation is enhanced with the increasing of H_2O_2 concentration. At pH 3, 1 mM H_2O_2 and current density

4.31 mA cm^{-2} after 60 minutes, dye degradation for 100 mg L^{-1} of Methylene blue and Titan yellow dye in solution was 98% and 96%, respectively.

Based on the kinetic studies a model prediction was developed. The experimental data showed a good fit to the theoretical model, which may be useful to scale up the process.

Our results prove that the pseudo-first order kinetic model is in good agreement with the experimental data. It was also noted that at a minimum current of 0.1 A, the energy requirement was lower, i.e., 1.14 kWh/kg COD removed. This reduced 68% COD for Methylene blue dye.

REFERENCES

1. A. K. Gupta, A. Pal and C. Sahoo, *Dyes Pigm.*, **69**, 224 (2006).
2. Q. Z. Dai, M. H. Zhou and L. C. Lei, *J. Hazard. Mater.*, **137**, 1870 (2006).
3. H. Lata, V. K. Garg and R. K. Gupta, *Dyes Pigm.*, **74**, 653 (2007).
4. X. S. Wang, Y. Zhou, Y. Jiang and C. Sun, *J. Hazard. Mater.*, **157**, 374 (2008).
5. V. K. Garg, M. Amita, R. Kumar and R. Gupta, *Dyes Pigm.*, **63**, 243 (2004).
6. T. Robinson, B. Chandran and P. Nigam, *Environ. Int.*, **28**, 29 (2002).
7. S. Wang, Y. Boyjoo and A. Choueib, *Chemosphere*, **60**, 1401 (2005).
8. O. Hamdaoui, *J. Hazard. Mater.*, **135**, 264 (2006).
9. C. S. Poon, Q. P. Huang and C. Fung, *Chemosphere*, **38**, 1005 (1999).
10. Y. B. Xie and X. Z. Li, *Mater. Chem. Phys.*, **95**, 39 (2006).
11. K. V. Kumar and A. Kumaran, *J. Biochem. Eng.*, **27**, 83 (2005).
12. D. Ozer, G. Dursun and A. Ozer, *J. Hazard. Mater.*, **144**, 171 (2007).
13. S. Papic, D. Vujevic, N. Koprivanac and D. Sinko, *J. Hazard. Mater.*, **164**, 1137 (2009).
14. Y. H. Huang, S. Chou, M. G. Perng, G. H. Huang and S. S. Cheng, *Water Sci. Technol.*, **39**, 145 (1999).
15. E. Brillas, J. C. Calpe and J. Casado, *Water Res.*, **34**, 2253 (2000).
16. S. H. Lin and C. C. Chang, *Water Res.*, **34**, 4243 (2000).
17. K. Cruz-Gonzalez, O. Torres-Lopez, A. Garcia-Leon, J. L. Guzman-Mar, L. H. Reyes, A. Hernandez-Ramirez and J. M. Peralta-Hernandez, *Chem. Eng. J.*, **160**, 199 (2010).
18. K. Juttner, U. Galla and H. Schmieder, *Electrochim. Acta*, **45**, 2575 (2000).
19. E. J. Ruiz, C. Arias, E. Brillas, A. Hernandez-Ramirez and J. M. Peralta-Hernandez, *Chemosphere*, **82**, 495 (2011).
20. C. A. Martinez-Huitle and E. Brillas, *Appl. Catal., B*, **87**, 105 (2009).
21. G. Q. Zhang, F. L. Yang, M. M. Gao, X. H. Fang and L. F. Liu, *Electrochim. Acta*, **53**, 5155 (2008).
22. D. Pletcher and F. C. Walsh, Industrial Electrochemistry, 2nd Ed., Chapman and Hall, London, UK (1990).
23. S. H. Lin and M. L. Chen, *Environ. Technol.*, **16**, 693 (1995).
24. S. H. Gau and F. S. Chang, *Wat. Sci. Technol.*, **34**, 455 (1996).
25. E. Brillas and J. Casado, *Chemosphere*, **47**, 241 (2002).
26. M. A. Oturan, J. Peiroten, P. Chartrin and A. J. Acher, *Environ. Sci. Technol.*, **34**, 3474 (2000).
27. M. Panizza and G. Cerisola, *Water Res.*, **35**, 3987 (2001).
28. A. Lahkimi, M. A. Oturan and N. Oturan, *Environ. Chem. Lett.*, **5**, 35 (2007).
29. E. Guivarch, S. Trevin, C. Lahitte and M. A. Oturan, *Environ. Chem. Lett.*, **1**, 38 (2003).
30. E. Rosales, M. Pazos, M. A. Longo and M. A. Sanroman, *Chem. Eng. J.*, **155**, 62 (2009).
31. N. Bensalah, M. A. Quiroz Alfaro and C. A. Martnez-Huitle, *Chem. Eng. J.*, **149**, 348 (2009).
32. M. Panizza and G. Cerisola, *Water Res.*, **43**, 339 (2009).
33. L. S. Clesceri, A. E. Greenberg and D. Andrew, Standard methods for the Examination of water and wastewater, 20th Ed., APHA, Washington, DC (1998).
34. I. Talini and G. K. Anderson, *Water Res.*, **26**, 107 (1992).
35. W. G. Kuo, *Water Res.*, **26**, 881 (1992).
36. P. Ghosh, A. N. Samanta and S. Ray, *Can. J. Chem. Eng.*, **88**, 1021 (2010).
37. M. Zhou, Q. Yu, L. Lei and G. Barton, *Sep. Purif. Technol.*, **57**, 380 (2007).
38. M. Zhou, Q. Yu and L. Lei, *Dyes Pigm.*, **77**, 129 (2008).
39. M. Pera-Titus, V. Garcia-Molina, M. A. Banos, J. Gimenez and S. Esplugas, *Appl. Catal. B: Environ.*, **47**, 219 (2004).
40. B. G. Kwon, D. S. Lee, N. Kang and J. Yoon, *Water Res.*, **33**, 2110 (1999).
41. A. M. El-Dein, J. A. Libra and U. Wiesmann, *Water Sci. Technol.*, **44**, 295 (2001).
42. J. H. Ramirez, F. M. Duarte, F. G. Martins, C. A. Costa and L. M. Madeira, *Chem. Eng. J.*, **148**, 394 (2009).
43. A. R. Khataee, V. Vatanpour and A. R. Amani Ghadim, *J. Hazard. Mater.*, **161**, 1225 (2009).
44. S. Altin, *Int. J. Chem. Reactor Eng.*, **9**, A33 (2011).
45. A. Altin, *Sep. Purif. Technol.*, **61**, 391 (2008).
46. C. T. Wang, J. L. Hu, W. L. Chou and Y. M. Kuo, *J. Hazard. Mater.*, **152**, 601 (2008).
47. E. Brillas, I. Sires and M. A. Oturan, *Chem. Rev.*, **109**, 6570 (2009).